The relationship between oscillatory EEG activity and the laminar-specific BOLD signal

René Scheeringa[a,1], Peter J. Koopmans[a,b], Tim van Mourik[a], Ole Jensen[a,c], and David G. Norris[a,d,e]

[a]Donders Institute for Brain Cognition and Behaviour, Radboud University, NL-6500 HB Nijmegen, The Netherlands; [b]Oxford Centre for Functional MRI of the Brain, University of Oxford, Oxford OX3 9DU, United Kingdom; [c]Center for Neuroscience, Swammerdam Institute for Life Sciences, University of Amsterdam, XH 1098 Amsterdam, The Netherlands; [d]Erwin L. Hahn Institute for Magnetic Resonance Imaging, D-45141 Essen, Germany; and [e]MIRA Institute for Biomedical Technology and Technical Medicine, University of Twente, NL-7500 AE Enschede, The Netherlands

Edited by Nancy Kopell, Boston University, Boston, MA, and approved April 20, 2016 (received for review November 16, 2015)

Electrophysiological recordings in animals have indicated that visual cortex γ-band oscillatory activity is predominantly observed in superficial cortical layers, whereas α- and β-band activity is stronger in deep layers. These rhythms, as well as the different cortical layers, have also been closely related to feedforward and feedback streams of information. Recently, it has become possible to measure laminar activity in humans with high-resolution functional MRI (fMRI). In this study, we investigated whether these different frequency bands show a differential relation with the laminar-resolved blood-oxygen level-dependent (BOLD) signal by combining data from simultaneously recorded EEG and fMRI from the early visual cortex. Our visual attention paradigm allowed us to investigate how variations in strength over trials and variations in the attention effect over subjects relate to each other in both modalities. We demonstrate that γ-band EEG power correlates positively with the superficial layers' BOLD signal and that β-power is negatively correlated to deep layer BOLD and α-power to both deep and superficial layer BOLD. These results provide a neurophysiological basis for human laminar fMRI and link human EEG and high-resolution fMRI to systems-level neuroscience in animals.

cortical layers | oscillations | high-resolution fMRI | EEG

The different cortical layers have distinct anatomical connections with subcortical, upstream, and downstream cortical regions (1). Intracranial electrophysiological recordings in animals have linked neuronal oscillations in different frequency bands to the cortical feedforward and feedback information flow and to cortico-subcortical interactions (2–5). In line with these findings, electrophysiological recordings in animals have also demonstrated that changes in α-, β-, and γ-bands can be localized to specific cortical layers (6–12).

These findings are almost exclusively based on nonhuman animal research. Although a recent study explored the feasibility of measuring laminar-specific activity with magnetoencephalography (MEG) (13), most recent advances in measuring laminar activity in humans have been made using high-resolution functional MRI (fMRI) (14–18). In this study, we make use of these recent developments to investigate the relationship between electrophysiology and the laminar-specific blood oxygen level-dependent (BOLD) signal. By simultaneously measuring EEG and high-resolution fMRI in humans performing a visual attention task, we demonstrate that changes in specific frequency bands in the EEG can be related to changes in the BOLD signal measured at different cortical depths.

The BOLD signal is thought to be closely related to variations in local field potentials (19–21). A wide variety of features in the local field potential (LFP) or EEG, related to several cognitive processes, have now been found to correlate with the BOLD signal (19, 20, 22–26). Most relevant for this study, α- and β-power changes in EEG correlate negatively with the BOLD signal whereas γ-band changes have a positive relation (20, 22–24, 27). Moreover, we and others have demonstrated that neuronal dynamics underlying changes in power in the γ-range contribute independently to the BOLD signal from those in the α- and β-bands (22, 27).

The visual attention paradigm we use in this study was adapted from an earlier study in which we observed that the neural processes related to γ-band and α-/β-band EEG power independently contribute to the BOLD signal (27). In this paradigm (Fig. 1*A*), subjects are presented with a cue that indicates whether a speed increase in a subsequent inward contracting circular sinusoid grating, lasting maximally 1,600 ms, is likely to occur ("attention-on," 75% of trials), or will not occur ("attention-off," 25%). In two thirds of the attention-on trials, a speed increase requiring a button press occurred after either 1,200 ms or 1,400 ms. This contracting grating reliably induced decreases in α- and β-band power and an increase in γ-band power at single subject level in both EEG and MEG (27, 28). From MEG source analysis and intracranial recordings in monkeys using this paradigm or similar paradigms, we know that these changes in α-, β-, and γ-band activity originate from early visual cortices (28–30) and overlap with fMRI activation (28). This paradigm therefore links findings across species and measurement modalities (31). These earlier findings make this task well-suited to investigate how variations in EEG power in the different frequency bands relate to the BOLD signal measured at varying cortical depths.

During the task, EEG and high-resolution fMRI (0.75 mm isotropic) were measured in an interleaved fashion (EEG was measured in between the acquisition of fMRI volumes), making use of the fact that the BOLD response lags neural activity by several seconds (Fig. 1*B*). This approach avoids large artifacts related to MR gradients in the EEG during the trial that will strongly affect the γ-band. The setup allowed us to correlate trial-by-trial fluctuations in

Significance

In this study, we demonstrate that α-, β-, and γ-oscillations can be related to activity in different cortical layers in the human brain. These cortical layers are believed to instantiate feedforward and feedback information streams. Electrophysiological oscillations in α- (8–12 Hz), β- (15–30 Hz), and γ- (40–100 Hz) bands have also been associated with different roles in feedforward and feedback processes and to different cortical layers in nonhuman animals. By simultaneously recording laminar functional MRI (fMRI) and EEG, we could directly link oscillatory signals to activity in cortical layers in humans. This research provides an important neural basis for noninvasive research into the role of cortical layers in information processing using laminar fMRI alone or combined with EEG.

Author contributions: R.S., P.J.K., O.J., and D.G.N. designed research; R.S. and P.J.K. performed research; P.J.K. and T.v.M. contributed new reagents/analytic tools; R.S., P.J.K., and T.v.M. analyzed data; and R.S., P.J.K., T.v.M., O.J., and D.G.N. wrote the paper.

The authors declare no conflict of interest.

This article is a PNAS Direct Submission.

[1]To whom correspondence should be addressed. Email: rene.scheeringa@donders.ru.nl.

This article contains supporting information online at www.pnas.org/lookup/suppl/doi:10.1073/pnas.1522577113/-/DCSupplemental.

NEUROSCIENCE

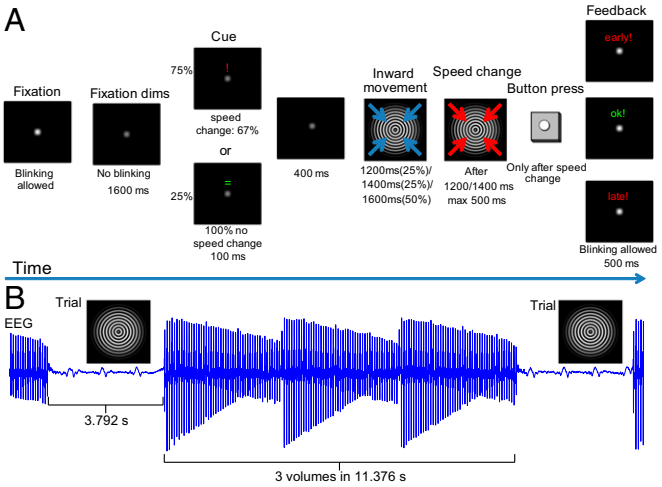

Fig. 1. (*A*) The paradigm. Each trial starts with the dimming of a fixation point instructing the subject to stop blinking. After 1,600 ms, a cue (100 ms) is presented informing subjects whether or not a speed change is likely to occur. When cued (75% of the trials), a speed change followed in 66.7% of the trials. A speed change never occurred when not indicated (25%). After a cue, there is a 400-ms pause, after which the fixation point is replaced by a contracting grating. When cued, a speed increase could occur after 1,200 ms (33.3% of these trials) or 1,400 ms (33.3%) from the start of the contracting grating. Subjects were instructed to push a button as soon as they detected it. The grating stopped contracting as soon as the button was pressed, or otherwise after 500 ms. Visual stimulation lasted for 1,600 ms in trials without a speed change in either condition. Feedback was given for 500 ms. (*B*) The timing of the trials relative to fMRI data acquisition. The trial was presented after every third echo-planar imaging (EPI) volume (acquisition time, 3.792 s per volume) in a scan-free period that also lasted for 3.792 s.

power for frequencies up to 120 Hz with trial-by-trial fluctuations in the laminar-specific BOLD signal in the early visual cortex (V1, V2, and V3). The attention manipulation consisted of attention-on versus attention-off conditions. This simple manipulation modulated not only attention but also other factors, like the expectation or predictability of the speed change. It was chosen to maximally modulate the α-, β-, and γ-band responses and consequently increase the likelihood of observing laminar-specific correlations over subjects.

Results

Basic Task Effects. We first describe the basic task effects that formed the basis for our integrated EEG–fMRI analysis. Our experimental paradigm is depicted in Fig. 1 (*Supporting Information*). Analysis of the behavioral data obtained showed that subjects correctly responded or withheld their response on average in ∼93% of the trials, indicating a good compliance with the task. The full behavioral results are described in Fig. S1. Previous electrophysiological studies using this task (27, 28, 32) have demonstrated stimulus-induced power changes in the α-, β-, and γ-bands over the occipital cortices. In the current experiment, we were able to replicate these results after applying a denoising strategy in which independent component analysis (ICA) unmixing weights were estimated on data bandpass-filtered in the γ-band (*Supporting Information*). The results of this strategy are depicted in Fig. 2*A* and demonstrate a clear power increase in the γ-band and decreases in the α- and β-bands when combining over attention conditions. These effects were present in 30 of 34 subjects (Fig. S2). The topographical representation in Fig. 2*B* demonstrates that the γ-band modulation dominated in posterior electrodes consistent with a source in the early visual cortex. For comparison, we repeated the analyses with an ICA denoising approach applied to 3- to 30-Hz bandpass-filtered data. As also reported in our previous work (27), this approach yielded similar results for the α-band, but not for the β- and γ-frequency bands (Fig. S3).

We also considered the attention modulation to correlate the attention effects in EEG power with the laminar-resolved BOLD signal over subjects in a frequency-specific manner. For this strategy to yield interpretable results, these attention effects should be present in both the electrophysiological and BOLD measurements. In the EEG data (Fig. 2*A*), we observed significant clusters 600 ms after onset of the visual stimulation until the end in the γ- (∼50–80 Hz) frequency band ($P < 0.0001$, corrected) (33) and in the low frequency range ($P < 0.0001$, corrected) extending over both the α- and β-bands. Within this large cluster, two regions of relatively strong effects, in terms of t values, were observed in the α-range (7.5–12.5 Hz) and the high β-range (22.5–26.25 Hz).

The laminar-resolved fMRI data consisted of 21 resampled laminar depths averaged over a cortical region. The laminar depths were equivolume linear interpolations between vertices indicating cerebrospinal fluid (CSF)–gray matter and white matter–CSF surfaces. We selected the 10% most-activated vertices from V1, V2, and V3 collapsed over the cortical depths (see Fig. 2*C* for an example subject). Fig. 2*D* clearly demonstrates that an attention effect at varying cortical depths can be observed for these selected vertices, which is a prerequisite for computing the correlation with the attention effects in EEG power. For the three visual regions combined (Fig. 2*D*, blue), there is a significant cluster including all cortical depths ($P = 0.001$). This result can also be observed for V1 (Fig. 2*D*, red) ($P = 0.001$) and V2 (Fig. 2*D*, pink) ($P = 0.001$). For V3 (Fig. 2*D*, cyan), the significant cluster includes only superficial and middle cortical depths ($P = 0.010$) although the effect is close to the cluster threshold for the deep layers.

Eye movements have been directly linked to visual LFP activity in the δ-/θ- and γ-bands (34) and across all cortical depths (35) whereas pupil dilation has been found to correlate negatively with

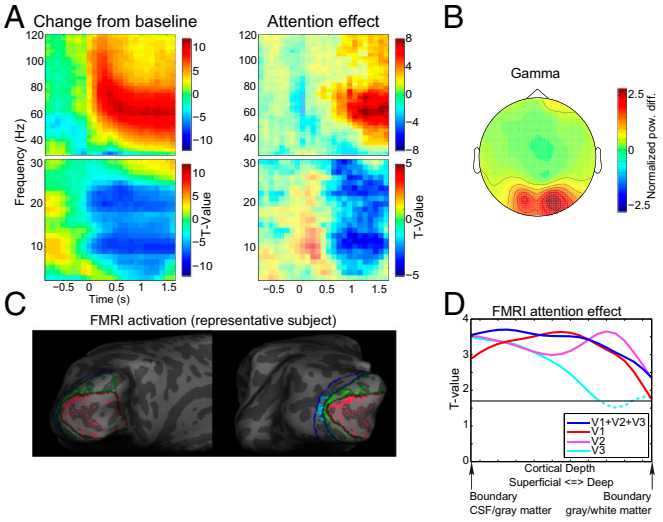

Fig. 2. Task-related EEG and fMRI effects. (*A*) Time-frequency representations of power relative to a pretrial baseline collapsed over the two attention conditions and as a contrast between the attention-on and attention-off conditions. Only trials with 1600-ms visual stimulation without a speed change were used for this representation. Separate time-frequency representations are shown for low (2.5–30Hz) and high (30-120 Hz) frequencies. (*B*) Average topography over subjects of the change in the γ-band from baseline. For each subject, the average power change from baseline in the range from 55 to 85 Hz during the visual stimulation period was computed and subsequently root-mean-square normalized over channels before averaging. (*C*) The 10% strongest activated vertices within the left hemisphere for V1 (red), V2 (green), and V3 (blue) for a representative subject. (*D*) Laminar-specific attention effect for the selected voxels over all subjects for V1, V2, and V3 combined, and separately.

the BOLD signal in the visual cortex (36). We recorded eye movements and pupil dilation to include these as possibly confounding or nuisance variables in the EEG–fMRI analysis. The full analyses of the eye movements and pupil dilation are described and discussed in *Supporting Information* and are shown in Figs. S4 and S5.

Integrated EEG and fMRI Analyses.

Trial-by-trial EEG–BOLD relation. We investigated the relationship between EEG power and the laminar-resolved BOLD signal by correlating the trial-by-trial variations in power with variations in the laminar-specific BOLD signal from the early visual cortex (V1, V2, and V3) (Fig. 3). We did this investigation in the context of the general linear model (GLM) in which we estimated a separate model for each cortical depth by frequency combination. The dependent variable was the laminar-specific BOLD signal. The first regressor in the design matrix consisted of an EEG power regressor that varied over frequencies. The other regressors in the design matrix that were fixed for all frequencies modeled the main task effects, task performance, pause-related T1 effect, eye movements, pupil dilation effect, and head motion. The EEG power regressor was derived by extracting single-trial power time courses for all correct artifact-free trials and convolving these with the standard hemodynamic response function implemented in SPM12. In the context of the task and confound regressors, this explains the variance in the BOLD signal related to trial-by-trial EEG power variations. The parameter estimates for the EEG power regressors in these GLMs form two (separate for low and high frequencies) frequency-by-cortical depth representations of how EEG power relates to the BOLD signal. In a first analysis, we combined the three early visual regions (Fig. 3*A*) and observed a cluster primarily in the α-range (7.5–12.5 Hz), stretching across all cortical depths showing a negative relation with the BOLD signal ($P = 0.001$), and a cluster in the γ-range (67.5–105 Hz) showing a positive relation with the BOLD signal at superficial and middle cortical depth ($P = 0.017$). For V1 ($P = 0.001$), V2 ($P = 0.002$), and V3 ($P = 0.003$), we observed the same effect for the α-band extending across all cortical depths whereas, for the γ-band, we observed a significant cluster at middle and superficial cortical depths only for V2 ($P = 0.021$) and V3 ($P = 0.009$) (Fig. 3 *B–D*). For V1, no significant cluster was observed ($P = 0.301$ for the largest cluster). These results clearly indicate a different profile over cortical depths of the EEG-power BOLD relation for α- and γ-band activity. These findings did not critically depend on the arbitrary percentage (5%, 10%, or 25%) of vertices selected (Fig. S6) and did not systematically differ between the attention conditions (Fig. S7).

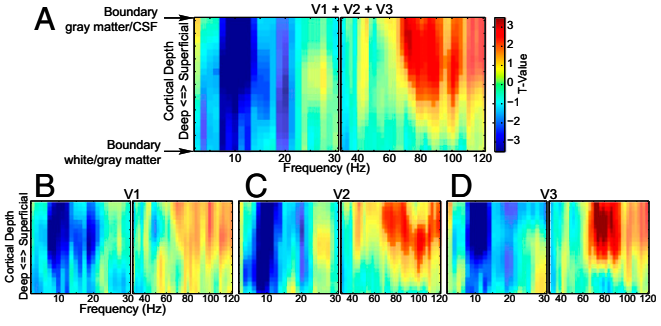

Fig. 3. Frequency by laminar depth representation of the relation between trial-by-trial variation in BOLD and EEG power. The results for V1, V2, and, V3 combined (*A*) and separately (*B–D*) are shown. High and low frequencies are depicted separately. The *t* values are based on single-sample *t* tests of the β-weights over subjects. Highlighted clusters are significant after correcting for multiple comparisons ($P < 0.05$).

We tested for a frequency-by-depth interaction in the EEG–BOLD relation, by assessing whether the profile for the α-band EEG–BOLD relation deviated from that from other frequencies (see *Supporting Information* for a more details). We observed (Fig. S8) that the α-profile significantly differed from the profile in the γ-range (65–107.5 Hz; $P = 0.004$) for the three regions combined and V2 ($P = 0.016$) and V3 separately ($P = 0.033$). As in our previous work (27), we found that the regressors for α- and γ-frequencies were uncorrelated (Fig. S9). The frequency by cortical depth interaction demonstrates that this absence of a correlation is related to different layer-specific neural processes and provides direct evidence for laminar-level sensitivity of high-resolution fMRI in relation to electrophysiological activity.

Attention effect. In the EEG, we observed attention effects in the α-, β-, and γ-bands, which were correlated with the attention effect in the BOLD signal across cortical depth for the three regions combined and separately. To correct for the potential confounding effect of the observed attention modulation in pupil dilation, we removed it from variations in both the EEG and fMRI attention effects by means of linear regression. The results are depicted in Fig. 4. For the three visual regions combined (Fig. 4*A*), the α-attention effect (Fig. 4, blue) significantly correlates with the BOLD attention effect at superficial depths ($P = 0.038$). For the β-band (Fig. 4, pink), a significant cluster is observed at lower depths ($P = 0.027$) whereas a significant cluster is observed at middle and superficial depths for the γ-band (Fig. 4, red) ($P = 0.015$).

For the individually tested regions (Fig. 4 *B–D*), we observed that the α-band correlations were strongest at superficial depths in all three regions. A significant cluster was found in superficial layers in V1 ($P = 0.033$) and V2 ($P = 0.031$). The cluster observed for V3 was not significant ($P = 0.071$). The β-band EEG attention effect correlated significantly with the laminar-specific attention effect of the BOLD signal at deeper cortical depths in V1 ($P = 0.019$) and V2 ($P = 0.022$). A cluster at the same depth for V3 was not significant ($P = 0.075$). For the γ-band, we observed no substantial difference in the correlation over cortical depths in V1: A significant cluster was observed for this region at middle cortical depths ($P = 0.010$), but it was close to the cluster threshold for all cortical depths. For V2 ($P = 0.026$) and V3 ($P = 0.012$), we observed robust correlations only for middle and superficial depths. In line with the different laminar profiles for the three frequency bands, no significant correlation between the attention effects was observed (Fig. S9).

Because these correlations were carried out on preselected frequency ranges, they could in theory be due to variations in wider frequency ranges (e.g., broadband changes) overlapping with the preselected frequency ranges where the attention effect was observed in the EEG. The analyses depicted in Fig. S10 show, however, that the observed correlations were limited to the frequency ranges that showed an attention effect in EEG power.

Control region. To test whether the patterns observed for the trial-by trial correlations and the attention effects were specific to visual regions, we performed the same analysis for nonactivated parts of the frontal cortex (Fig. S11). For this region, we observed a significant cluster with negative correlations covering all superficial depths only when considering the trial-by-trial analysis in the α-band. No other effects that were observed for early visual regions were found in the frontal cortex.

Discussion

In this study, we combined laminar-resolved fMRI and simultaneously recorded EEG in human subjects to investigate how BOLD activity measured from different cortical layers relates to frequency-specific power changes in the EEG. We observed an interaction between frequency and cortical depth in how trial-by-trial variation in EEG power relates to the BOLD signal. Although variation over trials in α-band power was related to the BOLD signal in both deep and superficial layers, γ-band activity showed a relation to the

NEUROSCIENCE

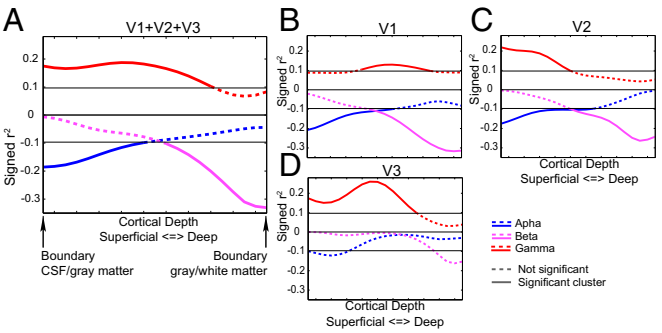

Fig. 4. Correlation of the attention effects in EEG power with the laminar-resolved attention effects in fMRI. The results for V1, V2, and, V3 both combined (*A*) and separately (*B–D*) are shown. The signed r^2 values plotted on the *y* axis are computed by multiplying the squared correlation with the sign of the correlation. Clusters significant after correcting for multiple comparisons ($P < 0.05$) are indicated with a solid line.

BOLD signal only at middle and superficial layers. This finding demonstrates that the BOLD signal at different cortical depths relates to different underlying neuronal dynamics. It supports our previous conclusion that the neural processes underlying α- and γ-band power variations independently contribute to changes in the BOLD signal (27). The observation that EEG power in different frequency bands is related to the BOLD signal at different cortical depths is strengthened by the correlation over subjects of the attention effects in EEG power and the cortical depth-resolved BOLD signal. This analysis shows clear laminar specificity in the three early visual regions for the attention effects observed in the α-, β-, and γ-bands. This work demonstrates that it is possible to link neuronal activity in different frequency bands as recorded by the EEG to laminar-resolved neural activity as measured by high-resolution fMRI. For laminar-level fMRI, our results strengthen the neurophysiological basis for conducting such studies.

Neuronal Basis of the BOLD Signal. Previous research on the neural basis of the BOLD signal has indicated that it is coupled to the power variations in the LFP (19–21). EEG, which we use here, as well as MEG and electrocorticography (ECoG), can be regarded as spatially macroscopic versions of the LFP. Human EEG and ECoG recordings combined with hemodynamic measurements have demonstrated that signals in the θ-, α-, and β-ranges are generally anticorrelated to the BOLD signal and that the γ-band signal is positively correlated with BOLD (22–24, 27, 32), which is in line with BOLD–LFP correlations in animals (20). In the current study, we extend these findings by quantifying the laminar contributions.

It is tempting to interpret the cortical depths at which EEG power correlates with the BOLD signal as the source location of the EEG rhythm. Because our results are correlational and the underlying sources of the observed EEG rhythms measured here are not known at the laminar level in advance, such a conclusion cannot be made directly. Any neuronal process that correlates with frequency-specific variation in EEG power and also results in a local (cortical depth-resolved) change in the BOLD signal can give rise to the results presented here. These processes are therefore not necessarily confined to the laminar source location of the EEG rhythm. The BOLD signal is thought to be primarily driven by excitatory (glutaminergic) synaptic activity in a voxel (37–39). Assuming that this activity is the cause of the BOLD signal, the results here can be interpreted as the relation between variation in frequency-specific EEG power originating from early visual cortex and laminar-specific changes in excitatory synaptic activity.

There are, however, some caveats to this interpretation. First, venous blood flows from deep to superficial layers in the cortex (40). As a result, BOLD activity and consequently EEG–BOLD relations observed in deeper layers can also spread to more superficial layers: like, for instance, the correlations we find in deep layers for α- and β-power. It is currently infeasible to measure the spatial point spread function of the BOLD response for activation of a single layer, because of the difficulty of stimulating a layer in isolation. Simulations have, however, shown that the BOLD response will peak in the stimulated layer and then exhibits a relatively flat tail of activation extending from the activated layer to the pial surface, with an amplitude of 20–25% of the peak activation (41). Significant activation is therefore most likely to be recorded in the activated layer and may be measured in more superficial layers depending upon the strength of the activation and the degree to which other layers also contribute; this is well-illustrated by the correlation of the attention effect over subjects in the β-band, which is strong in deep layers (~30% shared variance for V1), but close to zero for superficial depths.

Although we cannot claim that the cortical depths at which we find BOLD–EEG power correlations are the source of the observed EEG signals, we can compare the results with laminar-resolved electrophysiological recordings. In general, the correlation profiles for γ-band activity in the three regions combined (V1, V2, and V3) and also singly for V2 and V3 correspond well with laminar recordings in animals that have observed γ synchronization predominantly in the granular and supragranular layers of early visual regions (6, 7, 42). However, the correlations of the attention effects in V1 resulted in a flat profile over all cortical depths. Because studies mentioned above showed that γ-band synchronization in V1 is predominantly a supragranular effect, this finding suggests that neural processes reflected in the BOLD signal in all layers of V1 are related to the attention effect observed in γ with sources in superficial layers. A possible explanation for this result is that γ-band activity is coupled to excitatory bottom-up input from the lateral geniculate nucleus (LGN). Although the majority of these projections terminate in layer 4, some of these projections project to infragranular layers (1, 43). Furthermore it has been demonstrated that attention effects can be observed in the LGN in both animals (43–45) and humans (43, 46).

For the α-band, the correlations of variation over trials of BOLD and EEG power yielded a different picture than the corresponding correlation of the attention effects. Whereas the correlation over trials showed a significant negative correlation for all cortical depths, the correlation of the attention effects was observed only at superficial depths. This difference suggests multiple neural processes related to α-activity within the visual cortex as measured at the scalp with EEG. Although some studies have demonstrated multiple α-sources in the early visual regions in both supra- and infragranular layers (9, 12), others suggested a predominance of α-activity in deep layers (6, 11, 31). The results here are in line with multiple α-sources in both supra- and infragranular layers, in which, in our task, only the α-source or sources in more superficial layers are modulated by attention.

For the high β-band, we observed negative correlations over subjects of the attention affects only in deep layers. For the trial-by-trial correlation, we did not observe a correlation in the same frequency range. The results for this frequency band were, however, in line with previous findings that β-band EEG power is anticorrelated to the BOLD signal (24, 27) and is predominantly measured in the LFP recorded from infragranular layers in non-human animals (8). The deep layers are therefore also a likely source for the β-attention effect in the EEG measured here.

Eye movement-induced artifacts in the EEG have directly been linked to spurious γ-band power changes in the EEG (47). The results here, however, cannot be related to this artifact, and also an indirect route through neural activity related to eye movements or pupil dilation is unlikely. We discuss this theory in more detail in *Supporting Information* and Fig. S5.

Implications for Electrophysiological Research. Because the cortical layers have specific functions and connections with other cortical and subcortical brain regions, the technique described herein potentially allows us to link electrophysiological features measured by EEG to specific feedforward, feedback, and cortical–subcortical streams of information. We tentatively link the results for the different frequency bands in this experiment to laminar-specific electrophysiological and anatomical research.

The relationship we observed between the BOLD signal at middle and superficial depths and γ-band activity is in line with the notion that γ-oscillations are related to a bottom-up flow of information from lower to higher order cortical regions (2–4, 48). This bottom-up flow of information is thought to be mainly carried by intra- and interarea connections in granular and supragranular layers (2). In line with this theory, γ-oscillations are observed predominantly in granular and supragranular layers (6, 7, 10) and are thought to originate through an interaction of interneurons and pyramidal cells located in granular and supragranular layers (49, 50). For the β-band, we observed a negative correlation in deep layers that is particularly strong in V1 and V2. This finding corresponds with laminar recordings in animals that find the strongest β-band synchronization in deep layers (8). Furthermore, β-activity in early visual regions has been associated with top-down streams of information from higher order regions (2, 3, 48, 51).

We observed evidence for separate neural processes at deep and superficial cortical depths related to α-power. This finding is supported by laminar recordings in animals reporting both supra- and infragranular sources (9, 12) and relating α-activity to feedback projections that target both supra- and infragranular layers (4). Consistently, laminar fMRI work has linked feedback processes to both superficial (17) and deep layers (18). Interestingly, the attention modulation in the α-band is coupled to BOLD only in superficial layers. These layers are implicated in the bottom-up flow of information to higher order cortical regions. We have recently demonstrated that α-power in the early occipital cortex is also related to the routing of information to relevant higher order cortical regions (25) by inhibiting irrelevant information streams. This inhibition, reflected in lower α-power, is reduced for relevant information streams. The α-attention effect that is related to the BOLD attention effect in superficial layers might therefore reflect attentional control of the routing of information to downstream regions.

Our finding that α-oscillations are related to activity in deep layers agrees well with various laminar studies reporting α-activity in infragranular layers (6, 7, 9, 12). However, we did not find a relation between the attention effects in BOLD and α-power in the deep layers. Interestingly, we observed the inverse trial-by trial relation across all cortical depths also for the frontal cortex, which is likely not a generator of the measured α-activity. This result might therefore speak to a general effect throughout the cortex that is not modulated by our task. From intracranial animal work, we know that the phase of infragranular layer α can modulate supragranular γ-amplitude (11). This modulation has been linked to temporal coding and prioritizing visual processing (52) and might relate to visual sampling at roughly 10 Hz (53), supported by α-band synchronization between cortical regions. α-Band activity has been closely linked to thalamo-cortical loops (54), and α-band synchronization between regions is thought to be mediated through the pulvinar (43, 55). The trial-by-trial relation of α with BOLD across all layers might be observed throughout larger parts of the cortex through its dependence on loops involving through thalamic nuclei like the pulvinar.

General Conclusions

The integrated analysis of laminar-level fMRI and simultaneously recorded EEG is a previously unused methodological approach, and laminar level fMRI in humans is still a relatively young research field. As a consequence there are no standard analysis pipelines available yet for our approach. We therefore used the best techniques we had available at the time of writing.

The main aim of this study was to investigate whether EEG power from different frequency bands is differentially related to the cortical depth-resolved BOLD signal. In our opinion, this aim is convincingly demonstrated by the collection of results for the α-, β-, and γ-bands for both the correlation over trials as well as the correlation of the attention effect over subjects. With these results, we provide a neurophysiological basis for using high-resolution fMRI as a tool to investigate laminar processing in humans. These results also demonstrate that an accurate understanding of the neural activity underlying the cortical BOLD signal requires a detailed understanding of the cortical microcircuitry (56). In general, our findings correspond also well to what is known from laminar electrophysiological work in animals (6, 7, 9, 10, 12). Combining EEG and laminar fMRI therefore might prove a useful technique to link human cognitive neuroscience using fMRI and EEG/MEG to systems-level neuroscience approaches using animal models. The interpretations we provide for the laminar BOLD correlates of the different frequency bands warrant verification using other measurement modalities (e.g., intracranial and laminar recordings), brain regions, and experimental paradigms.

Materials and Methods

Thirty-four right-handed subjects (29 female, 5 male, mean age 21.6 y, range 18–26 y) without a history of known psychiatric or neurological disorders participated in the simultaneous EEG/fMRI session. Before the start of the experiment, written informed consent was obtained from each subject. The experiment was approved by the local ethical committee [Commissie Mensgebonden Onderzoek (CMO), region of Arnhem/Nijmegen, The Netherlands]. The results are based on thirty subjects with good quality EEG. Subjects performed a visual attention task (Fig. 1*A*) in three blocks of 72 trials. During the main task, we measured high-resolution fMRI data (3T; volume acquisition time, 3.792 s; 48 slices; resolution, 0.75 mm isotropic; 3.792 s pause after each third volume) and 64-channel EEG.

We estimated the cortical depth-resolved BOLD signal at 21 points in the gray matter between the boundaries with CSF and white matter for V1, V2, and V3. The average cortical depth-resolved signal per region was computed by averaging over the top 10% activated vertices (collapsed over cortical depth). To obtain clean estimates of power changes over a wide frequency range, we used an ICA-based denoising approach (27). Time-frequency analysis was carried out separately for a lower (2.5–30 Hz) and a higher (30–120 Hz) frequency window using a multitaper approach. Spectral changes in power relative to baseline, and between attention conditions, were computed.

We investigated the relationships between single trial variations in the cortical depth-resolved BOLD signal and EEG power, and between the cortical depth-resolved fMRI attention effect and the frequency-resolved EEG attention effect. For the analysis using single trial variations, separate general linear models were constructed for each frequency-cortical depth combination, resulting in a 2D depiction of the EEG–BOLD relation. We correlated the attention effects in power observed for the α-, β-, and γ-bands with the laminar-resolved attention effect in BOLD for the three visual regions. Statistical significance was assessed using a cluster-based randomization procedure (33).

The full methods section can be found in *Supporting Information*.

ACKNOWLEDGMENTS. This work was supported by the Netherlands Organization for Scientific Research by the VICI scheme 453-09-002 (to O.J.); the Netherlands Organization for Scientific Research by the Veni scheme 451-12-021 (to R.S.); and Wellcome Trust WT100092MA (to P.J.K.).

1. Douglas RJ, Martin KA (2004) Neuronal circuits of the neocortex. *Annu Rev Neurosci* 27:419–451.
2. Bastos AM, et al. (2015) Visual areas exert feedforward and feedback influences through distinct frequency channels. *Neuron* 85(2):390–401.
3. Bosman CA, et al. (2012) Attentional stimulus selection through selective synchronization between monkey visual areas. *Neuron* 75(5):875–888.
4. van Kerkoerle T, et al. (2014) Alpha and gamma oscillations characterize feedback and feedforward processing in monkey visual cortex. *Proc Natl Acad Sci USA* 111(40):14332–14341.
5. Saalmann YB, Pinsk MA, Wang L, Li X, Kastner S (2012) The pulvinar regulates information transmission between cortical areas based on attention demands. *Science* 337(6095):753–756.
6. Buffalo EA, Fries P, Landman R, Buschman TJ, Desimone R (2011) Laminar differences in gamma and alpha coherence in the ventral stream. *Proc Natl Acad Sci USA* 108(27):11262–11267.

7. Maier A, Adams GK, Aura C, Leopold DA (2010) Distinct superficial and deep laminar domains of activity in the visual cortex during rest and stimulation. *Front Syst Neurosci* 4:4.
8. Maier A, Aura CJ, Leopold DA (2011) Infragranular sources of sustained local field potential responses in macaque primary visual cortex. *J Neurosci* 31(6):1971–1980.
9. Bollimunta A, Mo J, Schroeder CE, Ding M (2011) Neuronal mechanisms and attentional modulation of corticothalamic α oscillations. *J Neurosci* 31(13):4935–4943.
10. Roberts MJ, et al. (2013) Robust gamma coherence between macaque V1 and V2 by dynamic frequency matching. *Neuron* 78(3):523–536.
11. Spaak E, Bonnefond M, Maier A, Leopold DA, Jensen O (2012) Layer-specific entrainment of γ-band neural activity by the α rhythm in monkey visual cortex. *Curr Biol* 22(24):2313–2318.
12. Haegens S, et al. (2015) Laminar profile and physiology of the α rhythm in primary visual, auditory, and somatosensory regions of neocortex. *J Neurosci* 35(42):14341–14352.
13. Troebinger L, López JD, Lutti A, Bestmann S, Barnes G (2014) Discrimination of cortical laminae using MEG. *Neuroimage* 102(Pt 2):885–893.
14. Koopmans PJ, Barth M, Norris DG (2010) Layer-specific BOLD activation in human V1. *Hum Brain Mapp* 31(9):1297–1304.
15. Polimeni JR, Fischl B, Greve DN, Wald LL (2010) Laminar analysis of 7T BOLD using an imposed spatial activation pattern in human V1. *Neuroimage* 52(4):1334–1346.
16. Huber L, et al. (2015) Cortical lamina-dependent blood volume changes in human brain at 7 T. *Neuroimage* 107:23–33.
17. Muckli L, et al. (2015) Contextual feedback to superficial layers of V1. *Curr Biol* 25(20): 2690–2695.
18. Kok P, Bains LJ, van Mourik T, Norris DG, de Lange FP (2016) Selective activation of the deep layers of the human primary visual cortex by top-down feedback. *Curr Biol* 26(3):371–376.
19. Logothetis NK, Pauls J, Augath M, Trinath T, Oeltermann A (2001) Neurophysiological investigation of the basis of the fMRI signal. *Nature* 412(6843):150–157.
20. Niessing J, et al. (2005) Hemodynamic signals correlate tightly with synchronized gamma oscillations. *Science* 309(5736):948–951.
21. Goense JB, Logothetis NK (2008) Neurophysiology of the BOLD fMRI signal in awake monkeys. *Curr Biol* 18(9):631–640.
22. Hermes D, et al. (2012) Neurophysiologic correlates of fMRI in human motor cortex. *Hum Brain Mapp* 33(7):1689–1699.
23. Scheeringa R, et al. (2009) Trial-by-trial coupling between EEG and BOLD identifies networks related to alpha and theta EEG power increases during working memory maintenance. *Neuroimage* 44(3):1224–1238.
24. Yuan H, et al. (2010) Negative covariation between task-related responses in alpha/beta-band activity and BOLD in human sensorimotor cortex: An EEG and fMRI study of motor imagery and movements. *Neuroimage* 49(3):2596–2606.
25. Zumer JM, Scheeringa R, Schoffelen JM, Norris DG, Jensen O (2014) Occipital alpha activity during stimulus processing gates the information flow to object-selective cortex. *PLoS Biol* 12(10):e1001965.
26. Debener S, Ullsperger M, Siegel M, Engel AK (2006) Single-trial EEG-fMRI reveals the dynamics of cognitive function. *Trends Cogn Sci* 10(12):558–563.
27. Scheeringa R, et al. (2011) Neuronal dynamics underlying high- and low-frequency EEG oscillations contribute independently to the human BOLD signal. *Neuron* 69(3): 572–583.
28. Hoogenboom N, Schoffelen JM, Oostenveld R, Parkes LM, Fries P (2006) Localizing human visual gamma-band activity in frequency, time and space. *Neuroimage* 29(3): 764–773.
29. Fries P, Reynolds JH, Rorie AE, Desimone R (2001) Modulation of oscillatory neuronal synchronization by selective visual attention. *Science* 291(5508):1560–1563.
30. Muthukumaraswamy SD, Singh KD (2008) Spatiotemporal frequency tuning of BOLD and gamma band MEG responses compared in primary visual cortex. *Neuroimage* 40(4):1552–1560.
31. Fries P, Scheeringa R, Oostenveld R (2008) Finding gamma. *Neuron* 58(3):303–305.
32. Koch SP, Werner P, Steinbrink J, Fries P, Obrig H (2009) Stimulus-induced and state-dependent sustained gamma activity is tightly coupled to the hemodynamic response in humans. *J Neurosci* 29(44):13962–13970.
33. Maris E, Oostenveld R (2007) Nonparametric statistical testing of EEG- and MEG-data. *J Neurosci Methods* 164(1):177–190.
34. Bosman CA, Womelsdorf T, Desimone R, Fries P (2009) A microsaccadic rhythm modulates gamma-band synchronization and behavior. *J Neurosci* 29(30):9471–9480.
35. Rajkai C, et al. (2008) Transient cortical excitation at the onset of visual fixation. *Cereb Cortex* 18(1):200–209.
36. Yellin D, Berkovich-Ohana A, Malach R (2015) Coupling between pupil fluctuations and resting-state fMRI uncovers a slow build-up of antagonistic responses in the human cortex. *Neuroimage* 106:414–427.
37. Hall CN, et al. (2014) Capillary pericytes regulate cerebral blood flow in health and disease. *Nature* 508(7494):55–60.
38. Lauritzen M, Mathiesen C, Schaefer K, Thomsen KJ (2012) Neuronal inhibition and excitation, and the dichotomic control of brain hemodynamic and oxygen responses. *Neuroimage* 62(2):1040–1050.
39. Lauritzen M (2005) Reading vascular changes in brain imaging: Is dendritic calcium the key? *Nat Rev Neurosci* 6(1):77–85.
40. Duvernoy HM, Delon S, Vannson JL (1981) Cortical blood vessels of the human brain. *Brain Res Bull* 7(5):519–579.
41. Markuerkiaga I, Barth M, Norris DG (2016) A cortical vascular model for examining the specificity of the laminar BOLD signal. *Neuroimage* 132:491–498.
42. Xing D, Yeh CI, Burns S, Shapley RM (2012) Laminar analysis of visually evoked activity in the primary visual cortex. *Proc Natl Acad Sci USA* 109(34):13871–13876.
43. Saalmann YB, Kastner S (2011) Cognitive and perceptual functions of the visual thalamus. *Neuron* 71(2):209–223.
44. McAlonan K, Cavanaugh J, Wurtz RH (2008) Guarding the gateway to cortex with attention in visual thalamus. *Nature* 456(7220):391–394.
45. Vanduffel W, Tootell RB, Orban GA (2000) Attention-dependent suppression of metabolic activity in the early stages of the macaque visual system. *Cereb Cortex* 10(2):109–126.
46. O'Connor DH, Fukui MM, Pinsk MA, Kastner S (2002) Attention modulates responses in the human lateral geniculate nucleus. *Nat Neurosci* 5(11):1203–1209.
47. Yuval-Greenberg S, Tomer O, Keren AS, Nelken I, Deouell LY (2008) Transient induced gamma-band response in EEG as a manifestation of miniature saccades. *Neuron* 58(3): 429–441.
48. Bastos AM, et al. (2012) Canonical microcircuits for predictive coding. *Neuron* 76(4): 695–711.
49. Börgers C, Epstein S, Kopell NJ (2005) Background gamma rhythmicity and attention in cortical local circuits: A computational study. *Proc Natl Acad Sci USA* 102(19): 7002–7007.
50. Hasenstaub A, et al. (2005) Inhibitory postsynaptic potentials carry synchronized frequency information in active cortical networks. *Neuron* 47(3):423–435.
51. Lee JH, Whittington MA, Kopell NJ (2013) Top-down beta rhythms support selective attention via interlaminar interaction: A model. *PLOS Comput Biol* 9(8):e1003164.
52. Jensen O, Gips B, Bergmann TO, Bonnefond M (2014) Temporal coding organized by coupled alpha and gamma oscillations prioritize visual processing. *Trends Neurosci* 37(7):357–369.
53. VanRullen R, Koch C (2003) Is perception discrete or continuous? *Trends Cogn Sci* 7(5): 207–213.
54. Hughes SW, Crunelli V (2005) Thalamic mechanisms of EEG alpha rhythms and their pathological implications. *Neuroscientist* 11(4):357–372.
55. Lopes da Silva FH, Vos JE, Mooibroek J, Van Rotterdam A (1980) Relative contributions of intracortical and thalamo-cortical processes in the generation of alpha rhythms, revealed by partial coherence analysis. *Electroencephalogr Clin Neurophysiol* 50(5-6):449–456.
56. Logothetis NK (2008) What we can do and what we cannot do with fMRI. *Nature* 453(7197):869–878.
57. Marshall TR, Esterer S, Herring JD, Bergmann TO, Jensen O (October 9, 2015) On the relationship between cortical excitability and visual oscillatory responses: A concurrent tDCS-MEG study. *Neuroimage*, 10.1016/j.neuroimage.2015.09.069.
58. Muthukumaraswamy SD, Edden RA, Jones DK, Swettenham JB, Singh KD (2009) Resting GABA concentration predicts peak gamma frequency and fMRI amplitude in response to visual stimulation in humans. *Proc Natl Acad Sci USA* 106(20):8356–8361.
59. Muthukumaraswamy SD, Singh KD (2009) Functional decoupling of BOLD and gamma-band amplitudes in human primary visual cortex. *Hum Brain Mapp* 30(7): 2000–2007.
60. Poser BA, Koopmans PJ, Witzel T, Wald LL, Barth M (2010) Three dimensional echo-planar imaging at 7 Tesla. *Neuroimage* 51(1):261–266.
61. Koopmans PJ, Barth M, Orzada S, Norris DG (2011) Multi-echo fMRI of the cortical laminae in humans at 7 T. *Neuroimage* 56(3):1276–1285.
62. Dale AM, Fischl B, Sereno MI (1999) Cortical surface-based analysis. I. Segmentation and surface reconstruction. *Neuroimage* 9(2):179–194.
63. Fischl B, Sereno MI, Dale AM (1999) Cortical surface-based analysis. II. Inflation, flattening, and a surface-based coordinate system. *Neuroimage* 9(2):195–207.
64. Friston KJ, et al. (1995) Spatial registration and normalization of images. *Hum Brain Mapp* 3(3):165–189.
65. Greve DN, Fischl B (2009) Accurate and robust brain image alignment using boundary-based registration. *Neuroimage* 48(1):63–72.
66. Van Mourik T, Koopmans PJ, Norris DG (2015) Improved cortical boundary registration for locally distorted fMRI. *Proceedings of the ISMRM-ESMRBM Joint Annual Meeting 2014* (Curran Assoc, Red Hook, NY), p 903.
67. Kleinnijenhuis M, et al. (2015) Diffusion tensor characteristics of gyrencephaly using high resolution diffusion MRI in vivo at 7T. *Neuroimage* 109:378–387.
68. Bok S (1929) Der Einfluß der in den Furchen und Windungen auftretenden Krummungen der Großhirnrinde auf die Rindenarchitektur. *Z Gesamte Neurol Psychiatr* 12:682–750.
69. Waehnert MD, et al. (2014) Anatomically motivated modeling of cortical laminae. *Neuroimage* 93(Pt 2):210–220.
70. Oostenveld R, Fries P, Maris E, Schoffelen JM (2011) FieldTrip: Open source software for advanced analysis of MEG, EEG, and invasive electrophysiological data. *Comput Intell Neurosci* 2011:156869.
71. Hyvärinen A (1999) Fast and robust fixed-point algorithms for independent component analysis. *IEEE Trans Neural Netw* 10(3):626–634.
72. Mitra PP, Pesaran B (1999) Analysis of dynamic brain imaging data. *Biophys J* 76(2): 691–708.
73. Ashburner J, Friston KJ (2005) Unified segmentation. *Neuroimage* 26(3):839–851.
74. Wilcoxon F (1945) Individual comparisons by ranking methods. *Biom Bull* 1(6):80–83.